

Article

An Intelligent Control and a Model Predictive Control for a Single Landing Gear Equipped with a Magnetorheological Damper

Quang-Ngoc Le ^{1,†}, Hyeong-Mo Park ^{1,†}, Yeongjin Kim ^{1,*}, Huy-Hoang Pham ², Jai-Hyuk Hwang ³
and Quoc-Viet Luong ^{2,*}

¹ Department of Mechanical Engineering, Incheon National University, Incheon 22012, Republic of Korea; lqngoc@inu.ac.kr (Q.-N.L.); gudah52@inu.ac.kr (H.-M.P.)

² Faculty of Mechanical Technology, Ho Chi Minh City University of Industry and Trade, 140 Le Trong Tan Street, Tay Thanh Ward, Tan Phu District, Ho Chi Minh City 700000, Vietnam; hoangph@hufi.edu.vn

³ School of Aerospace and Mechanical Engineering, Korea Aerospace University, Goyang-si, Gyeonggi-do 10540, Republic of Korea; jhhwang@kau.ac.kr

* Correspondence: ykim@inu.ac.kr (Y.K.); vietlq@hufi.edu.vn (Q.-V.L.); Tel.: +84-782-725-699 (Q.-V.L.)

† These authors contributed equally to this work.

Abstract: Aircraft landing gear equipped with a magnetorheological (MR) damper is a semi-active system that contains nonlinear behavior, disturbances, uncertainties, and delay times that can have a huge impact on the landing's performance. To solve this problem, this paper adopts two types of controllers, which are an intelligent controller and a model predictive controller, for a landing gear equipped with an MR damper to improve the landing gear performance considering response time in different landing cases. A model predictive controller is built based on the mathematical model of the landing gear system. An intelligent controller based on a neural network is designed and trained using a greedy bandit algorithm to improve the shock absorber efficiency at different aircraft masses and sink speeds. In this MR damper, the response time is assumed to be constant at 20 ms, which is similar to the response time of the commercial MR damper. To verify the efficiency of the proposed controllers, numerical simulations compared with a passive damper and a skyhook controller in different landing cases are executed. The major finding indicates that the suggested controller performs better in various landing scenarios than other controllers in terms of shock absorber effectiveness and adaptability.

Keywords: magnetorheological damper; semi-active suspension; aircraft landing gear; greedy bandit algorithm; model predictive control; intelligent control; MR fluid



Citation: Le, Q.-N.; Park, H.-M.; Kim, Y.; Pham, H.-H.; Hwang, J.-H.; Luong, Q.-V. An Intelligent Control and a Model Predictive Control for a Single Landing Gear Equipped with a Magnetorheological Damper.

Aerospace **2023**, *10*, 951. <https://doi.org/10.3390/aerospace10110951>

Academic Editor: Gianpietro Di Rito

Received: 14 October 2023

Revised: 6 November 2023

Accepted: 9 November 2023

Published: 11 November 2023



Copyright: © 2023 by the authors. Licensee MDPI, Basel, Switzerland. This article is an open access article distributed under the terms and conditions of the Creative Commons Attribution (CC BY) license (<https://creativecommons.org/licenses/by/4.0/>).

1. Introduction

Magnetorheological (MR) dampers are generally used in many applications, such as architectural structures [1], car suspensions [2], and home applications [3,4]. Yet, applications in the aerospace domain are not common [5,6]. The advantage of the MR damper is that it has a simple structure by basically revising from the passive damper, and it is continuously controllable due to containing MR fluid [7]. However, three main challenges prevent MR dampers from being widely used in the aerospace industry, in particular landing gear applications. First, an MR damper is a complex nonlinear system. It always exhibits nonlinear hysteresis between its output force and relative velocity and nonlinear stiffness due to the state transition from liquid to semi-solid [8]. Second, the MR damper contains an unavoidable time delay [9] or response time [10]. The response time of the damper was identified in the range of 15–55 ms [11,12], which is not too short compared to the duration of the touchdown phase, which is about 50–200 ms. Thus, the response time may have a huge impact on the landing gear performance. Third, the aircraft must land in different landing cases, such as variable aircraft mass and sink speeds.

In an attempt to solve these problems, many researchers have successfully developed many controllers so far. For example, Yue Zhu and Sihong Zhu [13] developed a quarter-vehicle suspension equipped with an MR damper with a time delay using an adaptive neural network structure. Laihua Tao et al. [14] applied a Smith predictor-Taylor series-based LQG control to compensate for the time delay of a vehicle's semi-active suspension. Young-Tai Choi et al. analyzed MR dampers [15] and developed the controller for the landing gear system of a helicopter equipped with MR dampers. Yoon et al. [16] produced the force control based on the foundation of the optimal damping force. Jo et al. [17] applied two semi-active control algorithms, which are the skyhook control and hybrid control, to control the MR damper landing gear under various landing conditions. Knap et al. [18] developed a construction of a vehicle vibration damper controlled using a piezoelectric actuator that has a very small delay time of about 10 ms. So far, the control algorithm for landing gear in differing landing cases considering MR response time has not yet been invested. To deal with the MR response time, two types of controllers are the candidates: model predictive control (MPC) and intelligent controller based on reinforcement learning.

The advantage of MPC is that it computes a sequence of manipulated variable adjustments in order to optimize the future behavior of a plant [19]. An MPC algorithm computes a sequence of controlled variable adjustments for the future at each control interval in an effort to optimize plant behavior in the future. A solid introduction to the theoretical and practical challenges related to using MPC to deal with complex dynamic systems that contain time delays may be found in many recent papers. Mai et al. [20] presented the vibration control of a semi-active quarter-car suspension system equipped with a magneto-rheological damper that provides the physical constraint of a damping force. Dong et al. [21] introduced a gray skyhook prediction controller to compensate for the response time of magnetorheological semi-active seat suspension.

An intelligent controller based on reinforcement learning has been used to enable adaptive autonomy [22] and solve the optimization problem in autonomous control systems [23]. The concept of a full reinforcement learning algorithm, such as Q-learning and Sarsa, is that an agent improves its future action based on the long-term reward value of a pair of current states and actions [24]. The full reinforcement learning algorithm is developed based on the Markovian decision process, and it needs a big neural network to store all the reward values of all pairs of current state and action. A deep neural network is usually chosen in control systems [25]. A simple feedback reinforcement learning method is used as a bandit algorithm. This algorithm chooses the best action based on the history of all the past actions. So, the bandit algorithm can work well on the non-Markov chain system, and it requires a small neural network to link the state to the best action. Thus, the bandit algorithm is frequently encountered in various practical applications, such as recommender systems [26] and linear control systems [27].

The primary focus of this paper is to develop a simple controller that can improve the performance of a single landing gear equipped with an MR damper, which contains the response time in differing landing cases. In order to achieve this goal, a mathematical model of a landing gear system equipped with an MR damper is developed using MATLAB and then verified with the experimental data. Two types of controllers, a model predictive control and a simple bandit neural network controller, are then developed to compensate for the response time of the MR damper in differing landing cases.

The structure of the paper is arranged as follows: Section 2 shows the structure of a single landing gear equipped with the MR damper, and the mathematical model of our landing gear system is developed and verified; Section 3 explains the concept of the control design; Section 4 details the simulation results; and the conclusion is shown in Section 5.

2. Mathematical Model of the MR Damper

2.1. Structure of the Landing Gear Equipped with an MR Damper

In this paper, the structure of the landing gear is inspired by the work [17,28], as shown in Figure 1. The MR damper, which includes a piston, a cylinder, MR fluid, a floating

piston, and a gas accumulator, is the main component of the landing gear. The head of the piston divides the MR fluid-MRF-140CG, which is entirely injected into the MR damper, into upper and lower hydraulic chambers. This fluid from one chamber must pass through the orifices to the other chamber due to the piston action when the landing gear makes contact with the ground. It causes friction forces to develop within the vital fluid as well as between the fluid and the piston. Thus, when the landing gear makes contact with the ground, the landing energy can be smoothly absorbed. To account for the volume of the head piston caused by the piston's movement, pressurized air is built up inside the piston. Additionally, the compressed air serves as a spring, storing extra energy during the compression phase and releasing it during the ensuing extension period. The MR core, which houses the magnetic circuit, is inserted inside the piston's head. The electrical cable that exits the damper through a hole on the top of the cylinder carries electrical current to the MR core from the external electric board. Two wheels are symmetrically arranged on the landing gear to lessen the effect of friction force between the bearings and the piston.

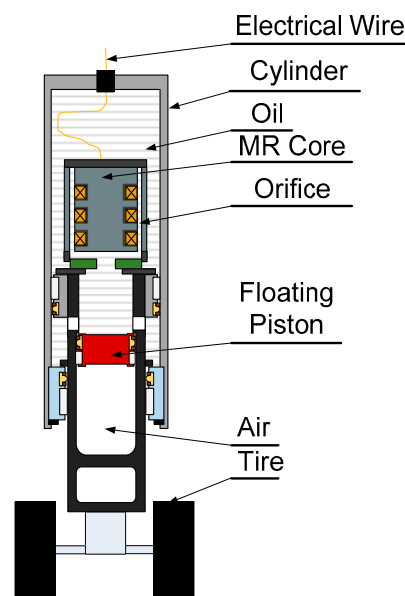


Figure 1. Landing gear's components [17].

2.2. Mathematical Model

The straightforward model of the landing gear during touchdown is detailed in the work [29]. It can be assumed that the upper and lower bodies of the landing gear move independently during touchdown, as can be seen in Figure 2. Consequently, the dynamic landing gear system's equations of motion are as follows [30]:

$$m_1 \ddot{z}_1 = m_1 g - F_a - F_v - F_{MR} \quad (1)$$

$$m_2 \ddot{z}_2 = m_2 g + F_a + F_v + F_{MR} - F_T \quad (2)$$

$$z_1(t=0) = z_2(t=0) = 0, \dot{z}_1(t=0) = \dot{z}_2(t=0) = v \quad (3)$$

where z_1 and z_2 are the displacements of the aircraft and the wheel, respectively. For a closed system, the polytropic gas law is determined by the pneumatic force F_a :

$$F_a = A_p p_0 \left(\frac{V_0}{V_0 - A_p s} \right)^n \quad (4)$$

where $s = z_1 - z_2$ is the stroke. The viscous force F_v represents the viscous-induced stress or the Newtonian behavior of fluid as follows:

$$F_v = C\dot{s} \quad (5)$$

where C is the viscous co-efficiency. The tire force is the ground's reaction force to the tire and it indicates tire deformation:

$$F_T = k_T z_2^b \quad (6)$$

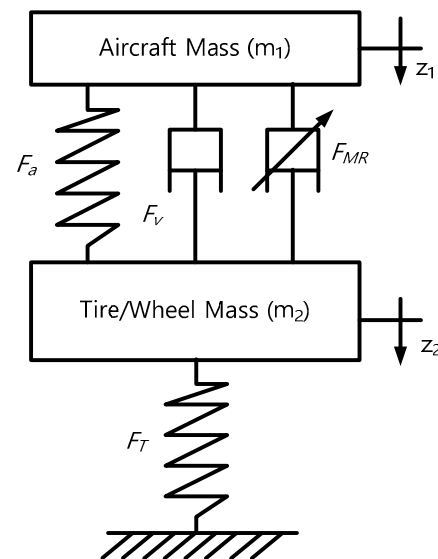


Figure 2. The model of landing gear with MR damper.

All parameters are given based on the work [17], as can be seen in Table 1. In that work, the authors executed many drop test experiments to find the characteristics of the landing gear. The specifics of the landing gear drop test experiment are displayed in Figure 3. The load cell, laser sensor, position sensor, accelerometer, and two pressure sensors are the five sensors that make up the drop test system. A dSPACE small box connected to a host PC running MATLAB Simulink was used to obtain the data. To retrieve the excitation signals and supply the MR damper with electrical current, the Simulink block was created. The comparison results of the mathematical model and the drop test experiment of the landing gear under the conditions of $m_1 = 245$ kg, and sink speed $v = 3$ m/s are given in Figure 4. It can be seen that there is a small error of under 5% between the results of the mathematical model and the experiments.

By adjusting the current supplied to the MR damper core from 0 A to 1 A at intervals of 0.25 A, the controlled force was determined. Figure 5 presents the findings. The control damping force increased with increasing electrical current; at 1 A of current, the maximum value of the MR force was observed at 1.7 kN.

The response time of the MR damper is defined as the required time to transition from the initial state of electrical current to 95% of the final state of the MR damper force [10]. The response time of an MR damper contains the response time of the magnetic circuit and the response time of the MR fluid [11]. The response time of MR fluid is very small, less than 1 ms, so it is assumed to be neglected. Thus, the main source of the response time of the MR damper is in the electrical circuit that generates the magnetic field from the input of the electrical current. It is difficult to determine the value of the response time due to the lack of equipment to measure the magnetic field. Thus, the response time of this research is

about 20 ms, which is similar to the response time of the commercial MR damper [31]. The response time of the MR damper can be described using the sigmoid function:

$$\text{sigmoid}(x) = \frac{1 - e^{-2x}}{1 + e^{-2x}} \tag{7}$$

The simulation result of the response time of the MR damper with variable applied electrical currents using the sigmoid function is shown in Figure 6. In our research, other delays, such as sensor and processor calculation delays, are assumed to be small; hence, they are assumed to be neglected. The sampling time is also chosen at 20 ms.

Table 1. The parameters of the landing gear system.

Symbol	Quantity	Value	Unit
A_p	cross-area of the head piston	2.1×10^{-3}	m^2
b	tire force index used to assess the nonlinearity of the tires	1.13	
C	viscous damping coefficient	9.77	kNs/m
g	gravitational acceleration	9.81	m/s^2
m_1	sprung mass (aircraft mass)	200–245	kg
m_2	un-sprung mass	18	kg
n	polytropic process index	1.3	
p_0	initial air chamber charging pressure	100	kPa
k_T	tire force constant	163	kN/m
v	initial sink speed of aircraft at touchdown	1.5–2.5	m/s
V_0	initial air chamber volume	4.26×10^{-4}	m^3
u	control input (electrical current)	0–1	A

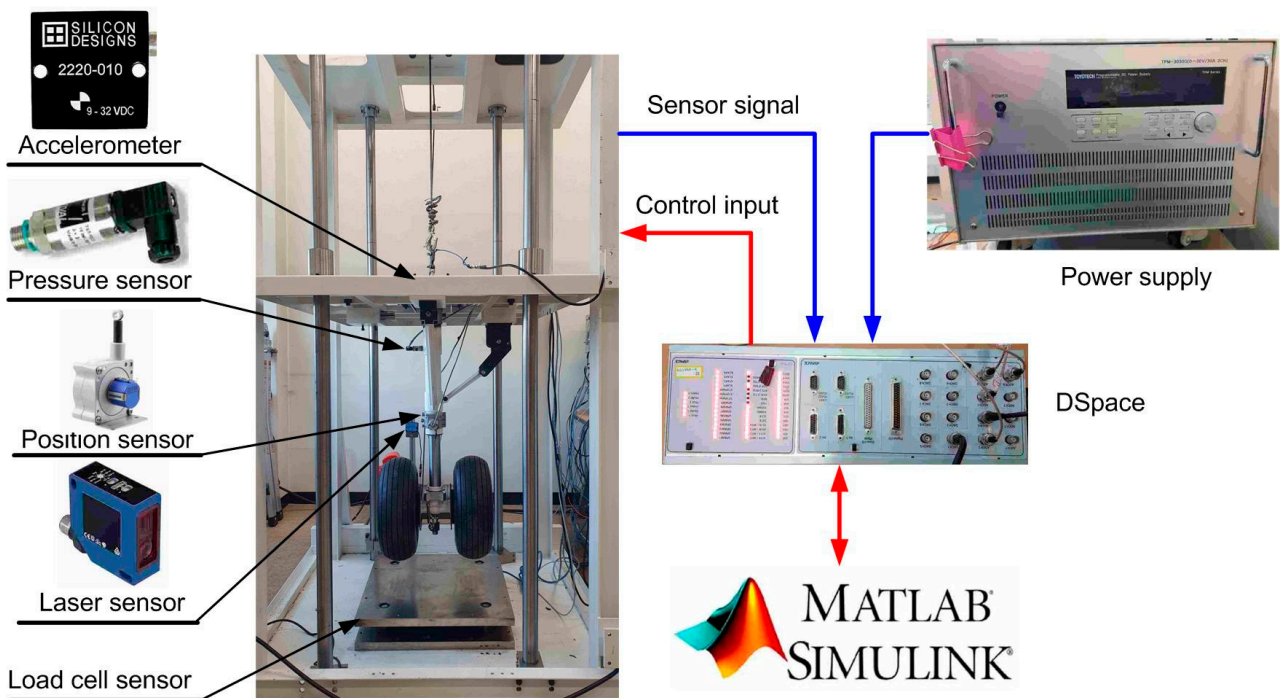


Figure 3. Drops test experiment [28].

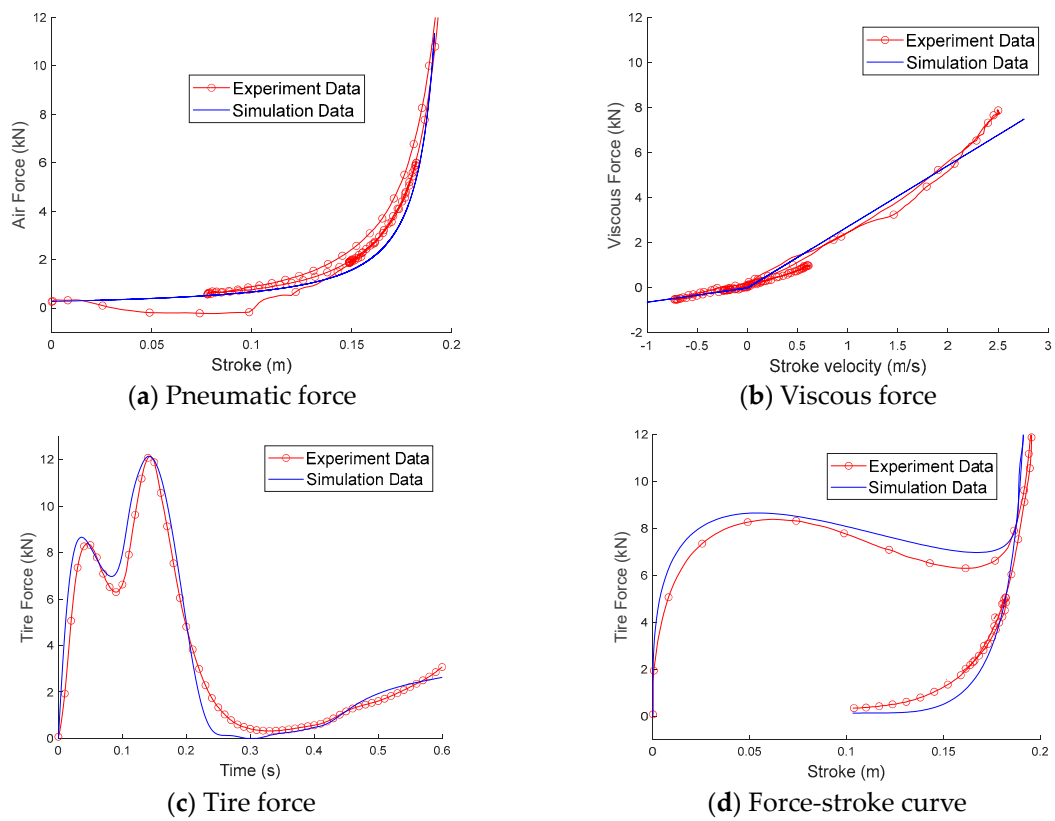


Figure 4. The comparison between experimental data and simulation results of landing gear in case of $m_1 = 245 \text{ kg}$, $v = 2.5 \text{ m/s}$.

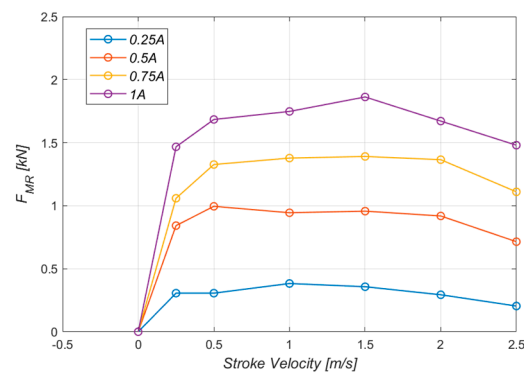


Figure 5. Controlled force F_{MR} .

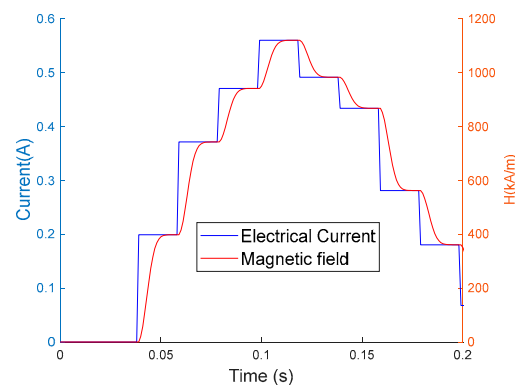


Figure 6. The behavior of the magnetic field.

3. Control Design

3.1. Control Target

Shock absorber efficiency is a metric unit to measure the percentage of the landing energy that is absorbed by a landing gear during the first stroke [32]. The shock absorber efficiency is calculated by the ratio between the total energy absorber of the landing gear during the first stroke and the product of maximum damping force (F_d^{max}) and maximum stroke (s^{max}). Thus, the shock absorber efficiency can be calculated by the following:

$$\eta = \frac{\int_0^{s^{max}} F_d ds}{s^{max} F_d^{max}} \tag{8}$$

where damping force $F_d = F_v + F_a + F_{MR}$. During touchdown, the landing gear must absorb all the potential and kinetic energy of the aircraft, as can be seen in the following example:

$$\int F_T dz_2 + \int F_d ds = (m_1 + m_2)gz_1 + \frac{1}{2}(m_1 + m_2)v^2 \tag{9}$$

In Equation (9), the right-hand side indicates the overall energy of the aircraft during touchdown, which is the kinetic and potential energy, while the left-hand side reflects the total energy that is absorbed by the landing gear system. Therefore, the aircraft mass and sink speed are the only two key variables that can alter this total energy. Moreover, the time delay is also the target of this research. So, the goal of the control is to improve the performance of the landing gear, which involves the time delay of the MR damper and various landing conditions. Or, the cost function of the control is to maximize the shock absorber efficiency in each of the landing cases in Table 2.

$$J = E(\eta) + w\Delta\eta \tag{10}$$

where

$$\begin{cases} E(\eta) = \frac{1}{9} \sum_{i=1}^9 \eta_i \\ \Delta\eta = \frac{1}{9} \sum_{i=1}^9 |\eta_i - E(\eta)| \end{cases} \tag{11}$$

and $w = -1$ is the scalar value.

Table 2. Shock absorber efficiency table.

		Aircraft Mass (kg)		
		200	225	245
Sink speed (m/s)	1.5	η_1	η_2	η_3
	2	η_4	η_5	η_6
	2.5	η_7	η_8	η_9

3.2. Model Predict Controller

MPC is a set of advanced control methods that explicitly use a model to predict the future behavior of the system [33]. The fundamental idea of MPC is illustrated in Figure 7. Based on the measurements made at time t , the controller forecasts the dynamic behavior of the system across a prediction horizon forward N steps in the future and chooses the input so that a specified open-loop performance objective is minimized (over a control horizon $t + N$). Normally, the target of MPC is to minimize the difference between the output of the system and the reference. In our proposed system, the main goal is to maximize the shock absorber efficiency, which is hard to achieve the goal of the MPC algorithm, as can be seen in Equation (10). So, the first step of the control design process is to find the approximate object function of the MPC.

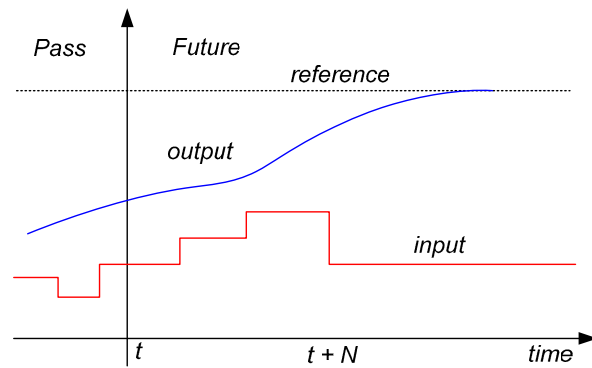


Figure 7. The concept of MPC.

From Equation (8), the aircraft landing gear achieves the maximum shock absorber efficiency when the numerator equals the denominator. So, the total energy of the aircraft during touchdown is seen to be rearranged into a rectangle that has a maximum constant damping force as its width. Thus, to improve the performance of the landing gear during touchdown, the idea of the control is to maintain the ideal maximum damping force (F_{target}) as long as possible during the first stroke, as can be seen in Figure 8 [30]. From Equation (9), under a landing condition (m_1, v), the right-hand side is constant. Moreover, the tire absorbs a small amount of energy, so the total energy that is absorbed by the damper is constant under a landing condition whether the MR damper is used or not. Thus, the target damping force is calculated based on the performance of the passive damper:

$$F_{target} = \frac{\int F_{d,passive} ds}{s_{ideal}} \tag{12}$$

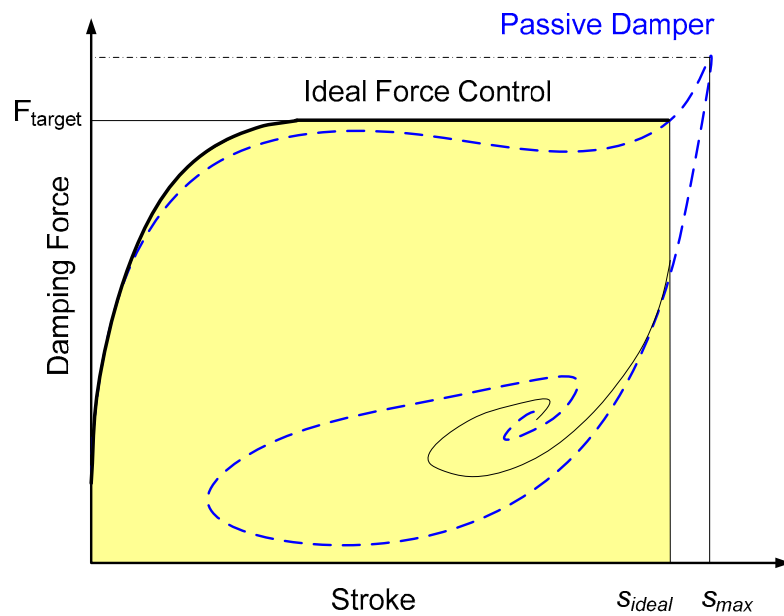


Figure 8. The concept of ideal force control [30].

The numerator in Equation (12) represents the total energy of a passive damper. The total energy of the ideal control is the area of the rectangle that has a width of F_{target} and a length $s_{ideal} \approx 0.9s_{max}$. The values of F_{target} under various landing conditions are given in Figure 9.

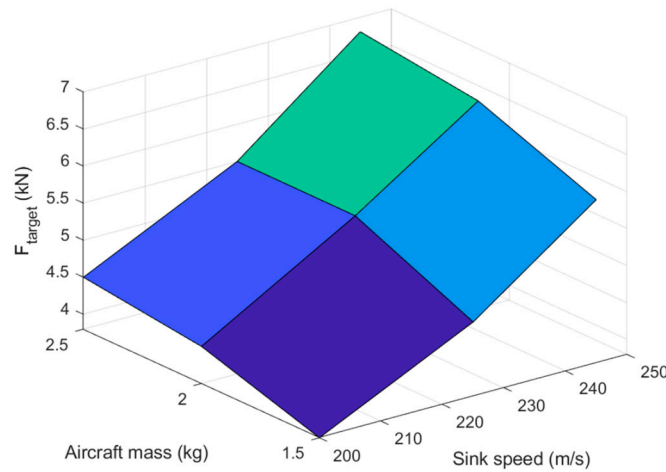


Figure 9. The F_{target} under various landing conditions.

The MPC is designed to drive the MR damper following the F_{target} , so the cost function of MPC can be given as follows:

$$\begin{aligned}
 \text{Cost function} &= \int Er \, dt \\
 Er &= \begin{cases} 0, & F_{target} < F_d \\ F_{target} - F_d, & F_{target} \geq F_d \end{cases} \\
 0 &\leq u \leq 1
 \end{aligned} \tag{13}$$

In Equation (13), the semi-active condition has been applied. During the first stroke, the stroke velocity is always positive, so the MR damper cannot generate the negative following the semi-active condition. Thus, the MR damper turns off in case the damping force is less than the F_{target} .

The MPC algorithm is detailed in Figure 10. It can seem that at time t , after receiving the sensor signals, which are the potentiometer to measure stroke and the accelerometer to measure an aircraft’s acceleration, the MPC calculates N times forward the future control input based on the mathematical model, as

$$u_{MPC}(t) = \sum_{i=0}^N Er(i) \tag{14}$$

where i is the calculation step. The compensation damping force at step i is calculated based on Equation (13):

$$Er(i) = \begin{cases} 0, & F_{target} < \hat{F}_d(i) \\ F_{target} - \hat{F}_d(i), & F_{target} \geq \hat{F}_d(i) \end{cases} \tag{15}$$

where the estimation of damping force at step i is calculated based on Equations (4) and (5):

$$\hat{F}_d(i) = F_a + F_v + F_{MR}(i) \tag{16}$$

The initial MR force $F_{MR}(i) = 0$, and the MR force is calculated following Equation (16) at step i . Based on the mathematical model in Section 2.2, the future state of landing gear can be predicted following Equations (1)–(3). Assuming the control is calculated using a very strong computer that can solve the aircraft’s dynamic equation under 1 ms. Thus, the number of future steps N can be chosen by 20.

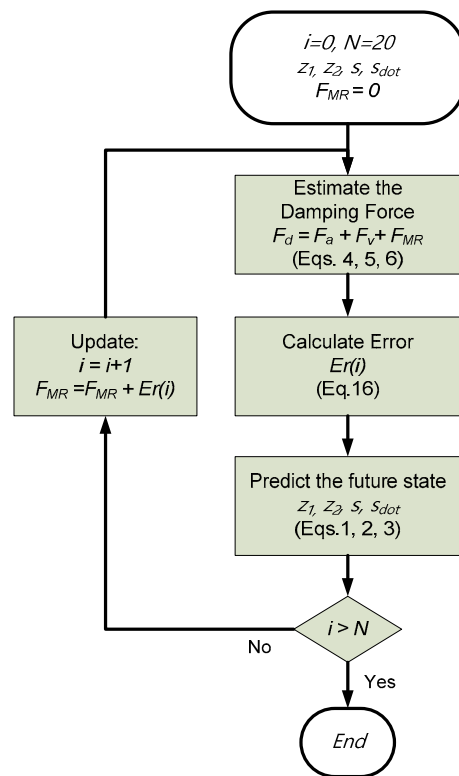


Figure 10. MPC schemes.

3.3. Bandit Neural Network Controller

An intelligent control based on the reinforcement neural network is the most famous control that can improve the system’s adaptive ability considering the unknown environment [34]. The concept of the intelligent controller involves two main parts, which are the structure of the neural network and the algorithm used to find the parameters in the neural network. The structure of the neural network is shown in Figure 11. As can be seen, there are only three inputs, which are stroke, stroke velocity, and aircraft acceleration, from two sensor signals. The output of the neural network is the electrical current, which is then applied to the MR damper. And there is only a hidden layer with ten neurals.

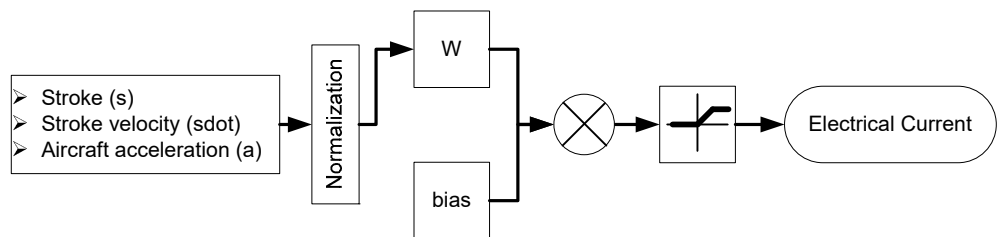


Figure 11. The concept of neural network.

$$Output = f(input \times W + bias)$$

$$f(x) = \begin{cases} 0, & x < 0 \\ x, & 1 \geq x \geq 0 \\ 1, & 1 > x \end{cases} \tag{17}$$

As mentioned before, the greedy bandit algorithm, which is a simple method in machine learning algorithms, is applied to find the optimal weight matrix and bias vector of the neural network. The concept of greedy bandit is shown below:

Initialization:

$$\begin{aligned}
 W_{max} &= 0 \\
 Q(0) &= 0 \\
 ki &= 0 \\
 P &= 0.5
 \end{aligned}
 \tag{18}$$

While looping until $Q(ki) \geq 0.9$ or $ki \geq 200$

$$W = \begin{cases} W_{max} & \text{with probability } 1 - P \\ W_{max} + 0.2 \times \text{rand}([0 \ 1]) & \text{with probability } P \end{cases}
 \tag{19}$$

$R \leq$ **bandit**(W):

If $J(W) > J(W_{max})$:

$$W_{max} = W$$

$$R = 0$$

else:

$$R = 0.9$$

$$\begin{aligned}
 Q(ki + 1) &= (ki + RQki) / ki \\
 ki &= ki + 1
 \end{aligned}
 \tag{20}$$

The algorithm only considers the weight matrix W_{max} , which has the maximum value of action $Q(ki)$. In the beginning, this weight matrix of the neural network is zero. The greedy algorithm is used to select exploiting or exploring actions. After exploiting actions, the agent will receive the maximum reward $R = 0.9$, which represents the maximum expected value of shock absorber efficiency. While exploring actions, the agent will be punished with $R = 0$ if the cost function $J(W)$ of the current weight matrix is larger than the cost function of $J(W_{max})$. The value of action $Q(ki)$ is then updated based on that reward, as can be seen in Equation (20). The algorithm converges when this value of action $Q(ki)$ reaches the maximum reward. The numerical simulation result of the greedy bandit algorithm is shown in Figure 12. It can be seen that the algorithm converges after more than 100 loops. The maximum value of the cost function is nearly 90%.

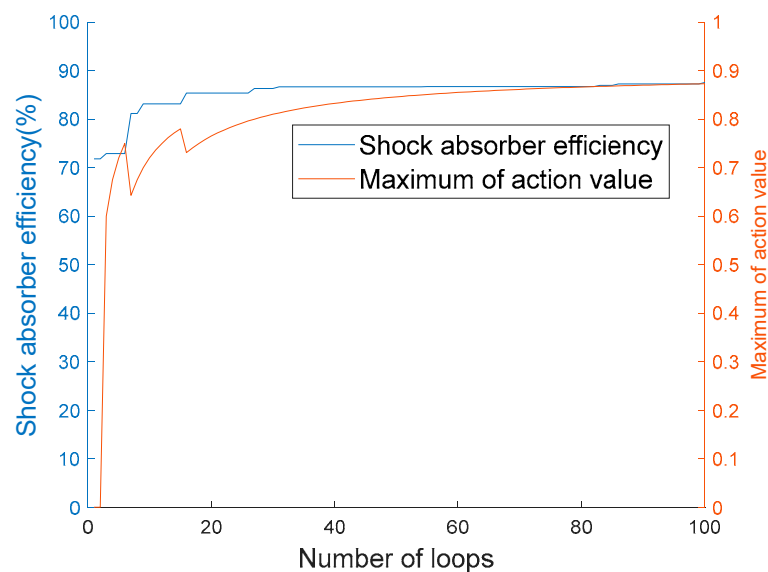


Figure 12. The simulation results of the greedy bandit algorithm.

4. Result and Discussion

To compare with the proposed controllers, the passive damper and skyhook controller are applied. The skyhook controller is the classical control that is used to control a suspension. The principle of skyhook control is given by the following:

$$u_{sky} = \begin{cases} C_{sky}\dot{z}_1, & \dot{z}_1\dot{s} > 0 \cup \dot{s} > 0 \\ 0, & elsewhere \end{cases} \quad (21)$$

where C_{sky} is the skyhook gain that is turned depending on the landing condition, as can be seen in Figure 13. In order to use that controller efficiently, the aircraft mass and sink speed are assumed to be known before touchdown.

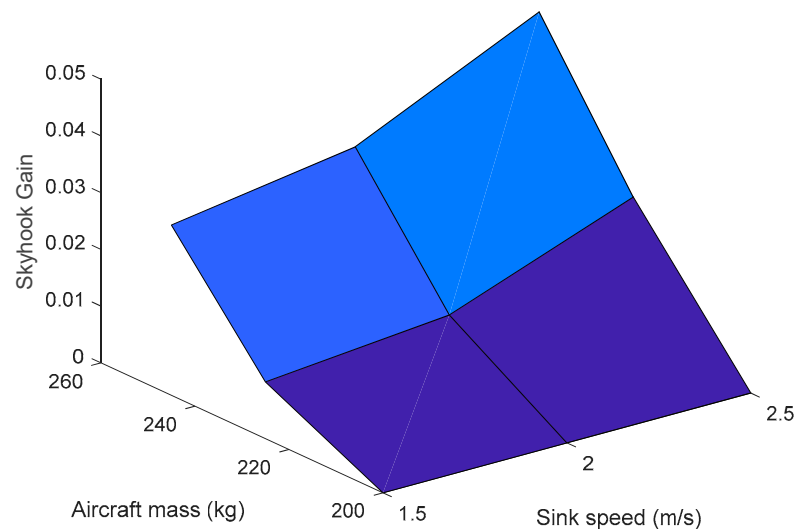


Figure 13. Skyhook gain surface.

To verify the efficiency of the proposed controllers, many numerical simulations are executed using MATLAB. Figure 14 shows a comparison of the landing gear performance of the passive damper, skyhook controller, MPC, and intelligent controller in the case of a heavy landing. As can be seen, the sampling time is 20 ms, so during the first stroke of about 150 ms, there are only seven control loops that are executed. The passive damper shows the highest tire force that can attach to the frame of the aircraft. All controllers dramatically reduce the maximum damping force. The proposed controllers exhibit better landing performance than that of other controllers. It produces the smallest stroke value, the smallest absolute aircraft acceleration, and the highest shock absorber efficiency. The MPC controller only predicted 20 steps forward in the future, while the intelligent controller simulated the whole system and chose the best action to claim the best cost function. So, the intelligent controller performed better than the MPC did. However, MPC can be executed online, whereas the intelligent controller must be trained offline based on several trials and errors.

Table 3 details the comparison of the shock absorber efficiency of landing gear using the passive damper, skyhook controller, and the proposed controllers at different aircraft mass and sink speeds. As can be seen, the proposed controllers also exhibit higher shock absorber efficiency than other controllers at various aircraft mass and sink speeds. In both the MPC and skyhook control, the landing conditions are assumed to be known, while the intelligent controllers do not require any knowledge of landing conditions. In order to verify the generalization ability of the proposed controllers, numerical simulations in the three random landing cases are executed, which are out of data training. Overall, the intelligent controller produced better adaptive ability than other controllers.

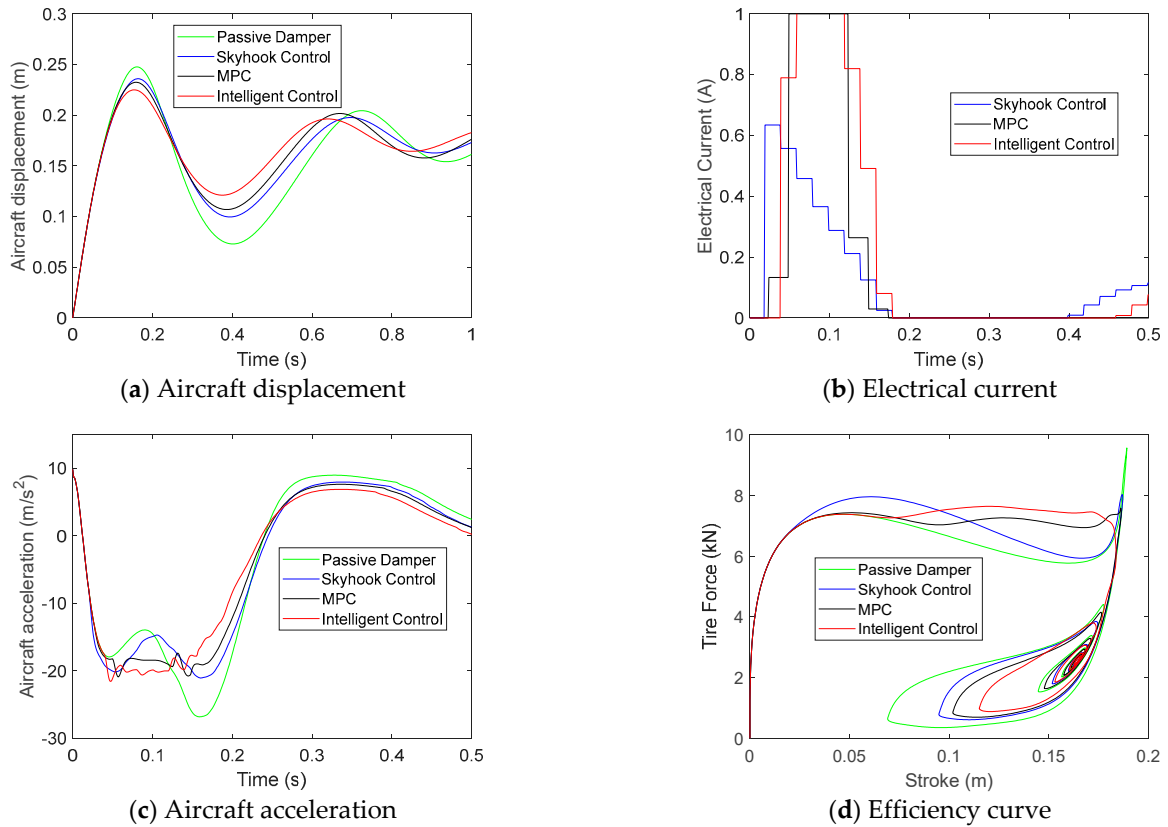


Figure 14. The performance of landing gear using the passive damper, skyhook control, MPC, and intelligent control in case of $m_1 = 245$ kg, $v = 2.5$ m/s.

Table 3. Damper performance using passive damping, skyhook control, MPC, and intelligent control in differing landing cases.

	Passive Damper			Skyhook Control			MPC			Intelligent Control		
	F_T^{max} (kN)	s^{max} (m)	η (%)	F_T^{max} (kN)	s^{max} (m)	η (%)	F_T^{max} (kN)	s^{max} (m)	η (%)	F_T^{max} (kN)	s^{max} (m)	η (%)
$m_1 = 200$ kg												
$v = 1.5$ m/s	4.72	0.172	79.5	4.72	0.172	79.5	4.72	0.166	81.0	4.72	0.162	82.3
$v = 2$ m/s	5.98	0.177	80.5	5.98	0.177	80.5	5.98	0.173	82.3	6.01	0.159	86.8
$v = 2.5$ m/s	7.26	0.183	82.8	7.26	0.183	82.8	7.26	0.180	84.9	7.45	0.166	89.0
$m_1 = 225$ kg												
$v = 1.5$ m/s	4.77	0.179	84.8	4.77	0.179	84.8	4.79	0.175	86.5	4.77	0.170	88.5
$v = 2$ m/s	6.85	0.183	85.0	6.85	0.183	85.0	6.04	0.179	87.9	6.05	0.172	91.2
$v = 2.5$ m/s	8.68	0.184	71.9	7.50	0.186	87.4	7.3	0.186	88.5	7.75	0.175	91.0
$m_1 = 245$ kg												
$v = 1.5$ m/s	5.82	0.183	73.2	5.13	0.180	84.8	5.53	0.169	87.5	4.81	0.176	92.9
$v = 2$ m/s	7.37	0.186	72.4	6.5	0.183	86.4	6.35	0.179	90.1	6.08	0.179	94.4
$v = 2.5$ m/s	9.55	0.189	68.3	8.05	0.186	87.2	8.04	0.180	92.6	7.54	0.184	95.2
$m_1 = 200$ kg (Random Case 1)												
$v = 2.25$ m/s	6.62	0.180	81.6	6.62	0.180	81.6	6.62	0.178	82.7	6.72	0.162	88.2
$m_2 = 225$ kg (Random Case 2)												
$v = 2.75$ m/s	9.18	0.189	75.6	8.32	0.187	86.2	8.65	0.183	87.9	8.20	0.182	93.8
$m_3 = 245$ kg (Random Case 3)												
$v = 1.75$ m/s	6.50	0.184	73.4	5.82	0.180	85.4	5.80	0.177	86.7	5.44	0.177	93.5

5. Conclusions

This paper adopted two types of control, which are MPC and intelligent control, for a single landing gear equipped with an MR damper in differing landing cases, considering the response time of the MR damper. Both the MPC and the intelligent controller required an accurate mathematical model for their design. So, the mathematical model of the landing gear touchdown dynamic is built and verified by the results of the drop test experiment. The MPC was built based on this mathematical model to reduce the effect of the time delay. An intelligent control based on the neural network was developed and trained using a greedy bandit algorithm. To verify the efficiency of the proposed controllers, many numerical simulations with different controllers, which are passive damper and skyhook control, in different landing scenarios were executed. Compared with other controllers, the proposed controllers have exhibited better shock absorber efficiency and also improved the adaptive ability of the landing gear system in different landing cases. In future work, the drop test experiment will then be set up to verify the efficiency of the proposed controller in the real case. Also, the controller will be developed to improve the robustness of the MR damper in different landing cases.

Author Contributions: Data curation, H.-M.P., Q.-V.L., Q.-N.L. and H.-H.P.; Formal analysis, H.-M.P., Q.-V.L., Q.-N.L. and Y.K.; Investigation, Y.K. and H.-H.P.; Methodology, H.-H.P. and J.-H.H.; Project administration, Y.K., Q.-V.L. and J.-H.H.; Software, H.-M.P., Q.-V.L. and Q.-N.L.; Supervision, Y.K. and J.-H.H.; Writing—original draft, Q.-V.L.; Writing—review and editing, H.-M.P., Q.-N.L., Y.K., H.-H.P. and J.-H.H. All authors have read and agreed to the published version of the manuscript.

Funding: This work was supported by the Incheon National University Research Grant in 2019.

Data Availability Statement: Data sharing is not applicable to this article.

Acknowledgments: The authors are very grateful for the support received from the Ho Chi Minh City University of Industry and Trade, Incheon National University, and Korea Aerospace University for this research.

Conflicts of Interest: The authors declare no conflict of interest.

References

1. Fallah, A.Y.; Taghikhany, T. Robust Semi-Active Control for Uncertain Structures and Smart Dampers. *Smart Mater. Struct.* **2014**, *23*, 095040. [[CrossRef](#)]
2. Oh, J.-S.; Choi, S.-B. Ride Quality Control of a Full Vehicle Suspension System Featuring Magnetorheological Dampers with Multiple Orifice Holes. *Front. Mater.* **2019**, *6*, 8. [[CrossRef](#)]
3. Chae, H.D.; Choi, S.-B. A New Vibration Isolation Bed Stage with Magnetorheological Dampers for Ambulance Vehicles. *Smart Mater. Struct.* **2015**, *24*, 017001. [[CrossRef](#)]
4. Bui, Q.-D.; Nguyen, Q.H.; Nguyen, T.T.; Mai, D.-D. Development of a Magnetorheological Damper with Self-Powered Ability for Washing Machines. *Appl. Sci.* **2020**, *10*, 4099. [[CrossRef](#)]
5. Choi, Y.-T.; Wereley, N.M. Vibration Control of a Landing Gear System Featuring Electrorheological/Magnetorheological Fluids. *J. Aircr.* **2003**, *40*, 432–439. [[CrossRef](#)]
6. Choi, Y.-T.; Robinson, R.; Hu, W.; Wereley, N.M.; Birchette, T.S.; Bolukbasi, A.O.; Woodhouse, J. Analysis and Control of a Magnetorheological Landing Gear System for a Helicopter. *J. Am. Helicopter Soc.* **2016**, *61*, 1–8. [[CrossRef](#)]
7. Choi, S.-B.; Han, Y.-M. *Magnetorheological Fluid Technology*; CRC Press: Boca Raton, FL, USA, 2012; ISBN 978-1-4398-5674-1.
8. Guo, D.L.; Hu, H.Y.; Yi, J.Q. Neural Network Control for a Semi-Active Vehicle Suspension with a Magnetorheological Damper. *J. Vib. Control* **2004**, *10*, 461–471. [[CrossRef](#)]
9. Strecker, Z.; Mazurek, I.; Roupec, J.; Klapka, M. Influence of MR Damper Response Time on Semiactive Suspension Control Efficiency. *Meccanica* **2015**, *50*, 1949–1959. [[CrossRef](#)]
10. Koo, J.-H.; Goncalves, F.D.; Ahmadian, M. A Comprehensive Analysis of the Response Time of MR Dampers. *Smart Mater. Struct.* **2006**, *15*, 351–358. [[CrossRef](#)]
11. Yoon, D.-S.; Park, Y.-J.; Choi, S.-B. An Eddy Current Effect on the Response Time of a Magnetorheological Damper: Analysis and Experimental Validation. *Mech. Syst. Signal Process.* **2019**, *127*, 136–158. [[CrossRef](#)]
12. Strecker, Z.; Roupec, J.; Mazurek, I.; Machacek, O.; Kubik, M.; Klapka, M. Design of Magnetorheological Damper with Short Time Response. *J. Intell. Mater. Syst. Struct.* **2015**, *26*, 1951–1958. [[CrossRef](#)]
13. Zhu, Y.; Zhu, S. Nonlinear Time-Delay Suspension Adaptive Neural Network Active Control. *Abstr. Appl. Anal.* **2014**, *2014*, 765871. [[CrossRef](#)]

14. Tao, L.; Chen, S.; Fang, G.; Zu, G. Smith Predictor-Taylor Series-Based LQG Control for Time Delay Compensation of Vehicle Semiactive Suspension. *Shock. Vib.* **2019**, *2019*, 3476826. [[CrossRef](#)]
15. Hong, S.-R.; John, S.; Wereley, N.M.; Choi, Y.-T.; Choi, S.-B. A Unifying Perspective on the Quasi-Steady Analysis of Magnetorheological Dampers. *J. Intell. Mater. Syst. Struct.* **2008**, *19*, 959–976. [[CrossRef](#)]
16. Yoon, J.-Y.; Kang, B.-H.; Kim, J.-H.; Choi, S.-B. New Control Logic Based on Mechanical Energy Conservation for Aircraft Landing Gear System with Magnetorheological Dampers. *Smart Mater. Struct.* **2020**, *29*, 084003. [[CrossRef](#)]
17. Jo, B.-H.; Jang, D.-S.; Hwang, J.-H.; Choi, Y.-H. Experimental Validation for the Performance of MR Damper Aircraft Landing Gear. *Aerospace* **2021**, *8*, 272. [[CrossRef](#)]
18. Knap, L.; Makowski, M.; Siczek, K.; Kubiak, P.; Mrowicki, A. Hydraulic Vehicle Damper Controlled by Piezoelectric Valve. *Sensors* **2023**, *23*, 2007. [[CrossRef](#)] [[PubMed](#)]
19. Qin, S.J.; Badgwell, T.A. A Survey of Industrial Model Predictive Control Technology. *Control Eng. Pract.* **2003**, *11*, 733–764. [[CrossRef](#)]
20. Mai, V.N.; Yoon, D.-S.; Choi, S.-B.; Kim, G.-W. Explicit Model Predictive Control of Semi-Active Suspension Systems with Magneto-Rheological Dampers Subject to Input Constraints. *J. Intell. Mater. Syst. Struct.* **2020**, *31*, 1157–1170. [[CrossRef](#)]
21. Dong, X.; Fei, Z.; Zhang, Z.; Deng, X.; Li, P.; Liu, Q. Gray Skyhook Predictive Control of Magnetorheological Semi-Active Seat Suspension with Time Delay. *Smart Mater. Struct.* **2023**, *32*, 115010. [[CrossRef](#)]
22. Kiumarsi, B.; Vamvoudakis, K.G.; Modares, H.; Lewis, F.L. Optimal and Autonomous Control Using Reinforcement Learning: A Survey. *IEEE Trans. Neural Netw. Learn. Syst.* **2018**, *29*, 2042–2062. [[CrossRef](#)] [[PubMed](#)]
23. Wang, Y.; Velswamy, K.; Huang, B. A Novel Approach to Feedback Control with Deep Reinforcement Learning. *IFAC-PapersOnLine* **2018**, *51*, 31–36. [[CrossRef](#)]
24. Konar, A. *Computational Intelligence*; Springer: Berlin/Heidelberg, Germany, 2005; ISBN 978-3-540-20898-3.
25. Mosavi, A.; Varkonyi, A. Learning in Robotics. *IJCA* **2017**, *157*, 8–11. [[CrossRef](#)]
26. Bouneffouf, D.; Rish, I. A Survey on Practical Applications of Multi-Armed and Contextual Bandits. *arXiv* **2019**, arXiv:1904.10040.
27. Cassel, A.; Koren, T. Bandit Linear Control. *Adv. Neural Inf. Process. Syst.* **2020**, *33*, 8872–8882.
28. Luong, Q.-V.; Jo, B.-H.; Hwang, J.-H.; Jang, D.-S. A Supervised Neural Network Control for Magnetorheological Damper in an Aircraft Landing Gear. *Appl. Sci.* **2021**, *12*, 400. [[CrossRef](#)]
29. Luong, Q.V.; Jang, D.-S.; Hwang, J.-H. Intelligent Control Based on a Neural Network for Aircraft Landing Gear with a Magnetorheological Damper in Different Landing Scenarios. *Appl. Sci.* **2020**, *10*, 5962. [[CrossRef](#)]
30. Luong, Q.V.; Jang, D.-S.; Hwang, J.-H. Robust Adaptive Control for an Aircraft Landing Gear Equipped with a Magnetorheological Damper. *Appl. Sci.* **2020**, *10*, 1459. [[CrossRef](#)]
31. Michal, K.; Ondřej, M.; Zbyněk, S.; Jakub, R.; Petr, N.; Ivan, M. Transient Magnetic Model of Magnetorheological Damper and Its Experimental Verification. *MATEC Web Conf.* **2018**, *153*, 06002. [[CrossRef](#)]
32. Currey, N.S. *Aircraft Landing Gear Design: Principles and Practices*; AIAA Education Series: United States of America; American Institute of Aeronautics and Astronautics: Washington, DC, USA, 1988; ISBN 0930403.
33. Schwenzer, M.; Ay, M.; Bergs, T.; Abel, D. Review on Model Predictive Control: An Engineering Perspective. *Int. J. Adv. Manuf. Technol.* **2021**, *117*, 1327–1349. [[CrossRef](#)]
34. Sutton, R.S.; Barto, A. *Reinforcement Learning: An Introduction*, 2nd ed.; Adaptive Computation and Machine Learning; The MIT Press: Cambridge, MA, USA; London, UK, 2020; ISBN 978-0-262-03924-6.

Disclaimer/Publisher’s Note: The statements, opinions and data contained in all publications are solely those of the individual author(s) and contributor(s) and not of MDPI and/or the editor(s). MDPI and/or the editor(s) disclaim responsibility for any injury to people or property resulting from any ideas, methods, instructions or products referred to in the content.